12th INTERNATIONAL SCIENTIFIC CONFERENCE ON DEFENSIVE TECHNOLOGIES
OTEH 2026
Serbia, Tara, 21 - 24 October 2026

DYNAMIC ANALYSIS OF 30 MM AUTOMATIC CANNON OPERATING MECHANISM

NIKOLA RADOVANOVIĆ
Military Technical Institute, Ratka Resanovića 1, 11000 Belgrade, Serbia
e-mail: nikola.radovanovic@mod.gov.rs

ALEKSANDAR KARI
Military Technical Institute, Ratka Resanovića 1, 11000 Belgrade, Serbia
e-mail: aleksandar.kari@mod.gov.rs

MILAN SIMONOVIĆ
Military Technical Institute, Ratka Resanovića 1, 11000 Belgrade, Serbia
e-mail: milan.simonovic@mod.gov.rs

MARKO SIMONOVIĆ
Military Technical Institute, Ratka Resanovića 1, 11000 Belgrade, Serbia
e-mail: marko.simonovic@mod.gov.rs

Abstract: *This paper presents a dynamic analysis of the operating mechanism of a 30 mm automatic cannon based on the gas-operated principle. By utilizing internal ballistics parameters obtained through the Drozdov method and the Bravin mathematical-mechanical model, a dynamic analysis of the bolt motion was performed. A MATLAB model of the 30 mm automatic cannon's bolt kinematics was developed, focusing on the dynamics during the recoil and counter-recoil cycles. This approach enabled the calculation of the theoretical rate of fire and illustrated the bolt velocity variations as a function of time. Finally, the obtained results were compared and validated against experimental data.*

Keywords: *30 mm automatic cannon, dynamic analysis, gas-operated mechanism, bolt kinematics, MATLAB modeling*

1. INTRODUCTION

A weapon based on the principle of gas operation is one that diverts part of the propellant gases through an opening in the barrel wall after the projectile passes that opening. This weapon uses the energy of the diverted gases to move the main assembly, which in turn drives all other parts of the weapon, while also accumulating energy in the return springs of the main assembly.

The device for diverting the propellant gases is most commonly called the gas regulator (gas piston system), and it consists of the following elements: the gas cylinder (often called the gas chamber), the working volume — the space into which the gas flows, ensuring the thermal process and the mechanical action of the gas — the gas port, a channel of various shapes through which the propellant gases pass from the barrel bore into the working volume of the gas regulator, the piston, which converts the gas action into kinetic energy, and the clearances and vent ports through which the propellant gases escape from the working volume, Fig. 1.

The problem of selecting the design parameters of the gas-operating system has given rise to a number of sub-variants of the piston-operated gas system: static, dynamic, static-dynamic, and others [1].

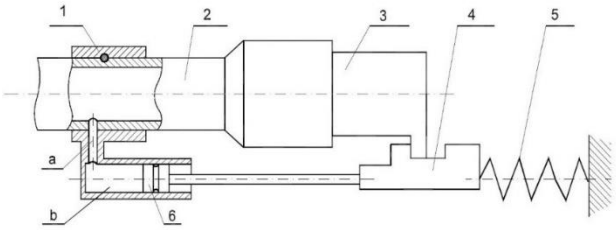


Figure 1. Diagram of automatic weapon based on the gas-operated principle
1-gas chamber, 2-barrel, 3-bolt, 4- bolt carrier, 5 – return spring, 6- piston, a- gas port, b – gas cylinder [2].

Figure 2 shows the characteristic variation of pressure in the gas regulator relative to the propellant gas pressure in the barrel, from the moment the projectile passes the gas port to the moment the outflow of the propellant gases ends.

The propellant gases behind the projectile, once its base passes the port, flow through the gas port and fill the cylinder containing the piston. The pressure of the diverted gas pushes the piston in the cylinder, so this work can be used to perform certain functions of the automatic weapon. This work is usually used to unlock the bolt or to actuate other automatic mechanisms.

Corresponding author: N. Radovanović;
E-mail: nikola.radovanovic@mod.gov.rs
DOI: 10.5937/OTEH26027R

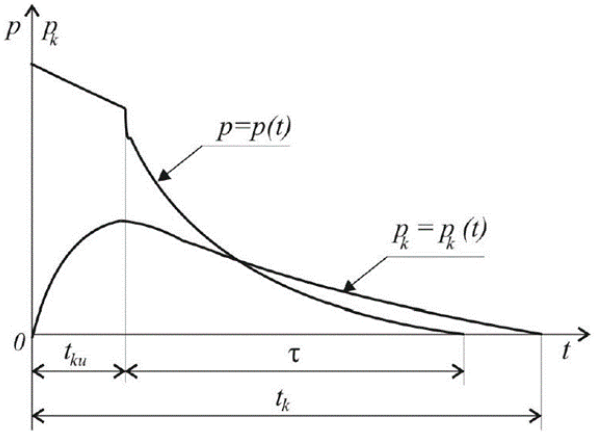


Figure 2. Pressure diagrams in the barrel and in the gas cylinder

The work of the diverted propellant gases can be used for various mechanisms, with the most common design solution being a cylinder with a piston and a piston rod for force transmission.

At the moment of firing, the bolt is firmly locked to the barrel. The force that propels the projectile and gases forward simultaneously acts on the case head in the opposite direction and produces recoil of the entire weapon.

When the projectile passes the gas port, the gases enter the gas port channel and generate a force on the gas piston.

The amount of gas required to move the piston is relatively small and does not significantly affect the muzzle velocity of the projectile.

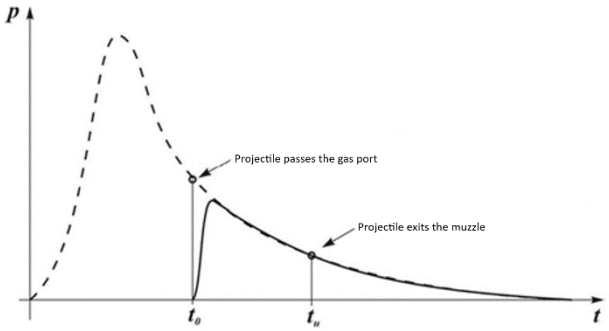


Figure 3. Propellant Gas Pressure Diagram

A piston with a larger effective area receives a greater impulse, and the magnitude of the impulse depends on the duration and magnitude of the gas pressure. This impulse depends directly on the size and shape of the port in the barrel wall. The magnitude of the piston energy depends on the piston mass, and for a given impulse, a piston of smaller mass has greater energy, since:

$$E = \frac{1}{2}mv^2 = \frac{1}{2}\frac{(mv)^2}{m} = \frac{1}{2}\frac{I^2}{m} \qquad (1)$$

In accordance with this, the influencing factors that determine the kinetic energy of the piston are:

- the pressure in the barrel,
- the position and size of the gas port,
- the cylinder diameter (shape of the port),
- the piston area and its mass [1] [3] [4].

2. PROPELLANT GAS PRESSURE

The internal ballistics calculation was performed using the Drozdov method. The Drozdov method is used for weapons that employ a single type of propellant. These include small arms, guns, and howitzers when firing charges made of only one type of propellant. This method is based on the analytical solution of the system of internal ballistics equations [5].

For the adopted propellant data and the structural characteristics of the barrel of the 30 mm automatic cannon, an internal ballistics calculation was performed, followed by optimization aimed at achieving a higher initial velocity and lower propellant gas pressure, and the final law of propellant gas pressure variation along the barrel as a function of the projectile's travel distance was obtained, Figure 4.

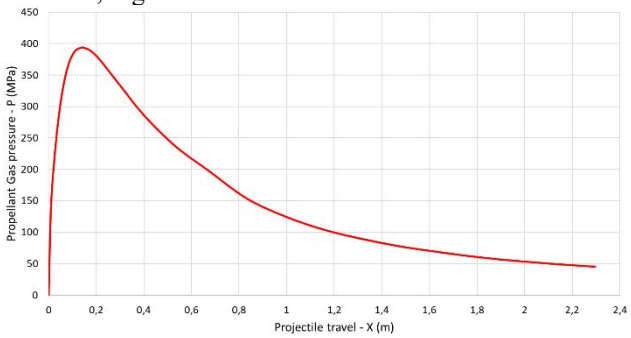


Figure 4. Optimized diagram of propellant gas pressure versus travel distance

Both domestic and foreign scientists have studied the examination of propellant gas pressures in gas regulators, with the aim of determining the law of variation *p=f(t)* and using that law to calculate the motion characteristics of the automatic weapon's main assembly. The problem of pressure in the gas regulator was addressed by Blagonravov A.A., Mamontov M.A., Bravin E.L., Paul Vieille, Jean Constantinet, Karl Becker, Hermann Scherer, Fiedner and Hutchings and others.

Bravin does not treat the process of gas outflow into the chamber as a thermodynamic process but instead offers an empirical expression for the propellant gas pressure in the gas chamber and on the piston of the main assembly, in order to represent as accurately as possible, the law of pressure variation of the gases entering the gas chamber [6].

As the basic factors influencing the law of propellant gas pressure variation on the piston, Bravin E.L.,[7] takes:

- the ratio of the cross-sectional areas of the gas port and the piston:

$$\sigma_0 = \frac{S_\phi}{S_n} \qquad (2)$$

- the transverse load of the piston:

$$K_0 = \frac{M_0}{S_n} \qquad (3)$$

In doing so, the following expression for the variation of gas pressure on the piston as a function of time is used:

$$p = p_\phi e^{-\frac{t}{b}}\left(1 - e^{-\alpha\frac{t}{b}}\right) \quad (4)$$

Where: $\alpha = n\frac{S_w M_w}{S_2^n}$; $b = \frac{i_0}{p_\phi}$; $i_0 = \frac{p_\phi + p_u}{2}t_n + \frac{p_u}{A}$

α – coefficient of useful action (efficiency);

b – Bravin's coefficient;

i_0 – unit impulse of the propellant gases in the barrel;

p_ϕ - the propellant gas pressure in the barrel bore at the moment the projectile passes the gas port;

p_u - the propellant gas pressure in the barrel bore at the moment the projectile exits the barrel;

$$\mathrm{A} = 0.365\frac{\beta^2}{\beta - 0.5} * \frac{\vartheta_0}{L'} \quad (5)$$

$$\beta = C\frac{d}{\vartheta_0}\sqrt{\frac{p_\partial L' g}{\omega}} \quad (6)$$

C – an experimental coefficient equal to $C = 1.5$

t_n - the time from the moment the projectile passes the gas port until it exits the barrel;

M_n - the mass of the automatic weapon's driving assembly

i_0 - the unit impulse of the propellant gas pressure in the barrel bore during time t_g

Then, for the unit (specific) impulse in the gas-operating device, we obtain:

$$i_k = \int_0^t p_\phi e^{-\frac{t}{b}}\left(t - e^{-\alpha\frac{t}{b}}\right)dt = \\ = p_\phi b\left[\frac{\alpha}{1+\alpha} + \frac{\alpha}{1+\alpha}e^{-(1+\alpha)\frac{t}{b}} - e^{-\frac{t}{b}}\right] \quad (7)$$

For $t \to \infty$ $i_k = p_\phi b\frac{1}{1+\alpha}$ where $\frac{\alpha}{1+\alpha} = \eta$

The quantity η represents the efficiency coefficient of the gas-operating system.

For $\eta = 1$ the entire pressure impulse in the barrel bore would be transferred to the piston without losses.

The total unit impulse in the barrel bore is:

$$i_0 = \frac{p_\phi + p_\partial}{2}t_n + \frac{p_\partial}{A} \quad (8)$$

гд where A is from equation (4),

then: $p_\phi b = i_0$ and $b = \frac{i}{p_\phi}$

In doing so, when $\alpha \to \infty$ the expression for the pressure in the gas chamber takes the form:

$$p = p_\phi e^{-\frac{t}{b}}\left(1 - e^{-\alpha\frac{i}{e}}\right) \quad (9)$$

For $\alpha \to \infty$:

$$p = p_\phi e^{-\frac{t}{b}} \quad (10)$$

and will represent the limiting family of curves:

$$p = p_\phi e^{-\frac{t}{e}}\left(1 - e^{-\alpha\frac{t}{b}}\right) \quad (11)$$

The dependence: $p = p_\phi e^{-\frac{t}{b}}$ can approximately express the law of pressure variation in the barrel bore after the projectile passes the gas port until the end of the period.

The impulse of the propellant gas pressure force on the piston is determined based on the expression:

$$S_n i_k = S_n\left(\frac{\alpha}{1+\alpha} + \frac{1}{1+\alpha}e^{-(1+\alpha)\frac{t}{b}} - e^{-\frac{t}{b}}\right)p_\phi b \quad (12)$$

But since $M_n V = S_n i_k$:

$$M_n V = S_n\left(\frac{\alpha}{1+\alpha} + \frac{1}{1+\alpha}e^{-(1+\alpha)\frac{t}{b}} - e^{-\frac{t}{b}}\right)p_\phi b \quad (13)$$

For $t \to \infty$: $M_n V = S_n\frac{\alpha}{1+\alpha}$; for $M_n = const$ the expression for $M_n V$ allows the velocity of the main assembly to be determined at any moment in time.

By integrating the expression for velocity, we obtain the expression for the displacement of the main assembly:

$$X = \int_0^x dX = \int_0^t V dt = \frac{S_n b}{M_n}\left(\frac{\alpha}{1+\alpha}\cdot\frac{t}{b} - \frac{\alpha(2+\alpha)}{(1+\alpha)^2} - \right. \\ \left. \frac{1}{(1+\alpha)^2}e^{-(1+\alpha)\frac{t}{b}} + e^{-\frac{t}{b}}\right)i_0 \quad (14)$$

For easier use of the expressions for determining p, V, X, coefficient tables have been formed:

$$K_p = e^{-\frac{t}{b}}\left(1 - e^{-\alpha\frac{t}{b}}\right) \quad (15)$$

$$K_v = \frac{\alpha}{1+\alpha} + \frac{1}{1+\alpha}e^{-(1+\alpha)\frac{t}{b}} - e^{-\frac{t}{b}} \quad (16)$$

$$K_x = \frac{\alpha}{1+\alpha}\cdot\frac{t}{b} - \frac{\alpha(2+\alpha)}{(1+\alpha)^2} - \frac{1}{(1+\alpha)^2}e^{-(1+\alpha)\frac{t}{b}} \\ + e^{-\frac{t}{b}} \quad (17)$$

Then we obtain:

$$p = p_\phi K_p \quad (18)$$

$$V = \frac{S_n i_0}{M_n}K_v \quad (19)$$

$$X = \frac{S_n b i_0}{M_n}K_x = \frac{Vb}{K_v}K_x \quad (20)$$

To determine the quantity $\eta_k = \frac{\alpha}{1+\alpha}\eta_0 v_0 v_g v_{g0}$ dependency tables have been formed

$$\eta_0 = f(\sigma_\Pi, \sigma_\Delta)$$
$$v_0 = f(\sigma_\Pi, \sigma_0)$$
$$v_g = f(\sigma_\Pi, \sigma_g)$$
$$v_{g0} = f(\sigma_0, \sigma_g)$$

The stated tables for determining the impulse efficiency coefficients can be used to calculate the pressure and motion characteristics of the automatic weapon's main assembly during its free travel, both according to the method of Mamontov M.A. and according to the method of Bravin E.L. [6] [7].

For the purpose of simulating the pressure in the gas

cylinder, a software solution was developed in MATLAB, whose algorithm is shown in Figure 5.

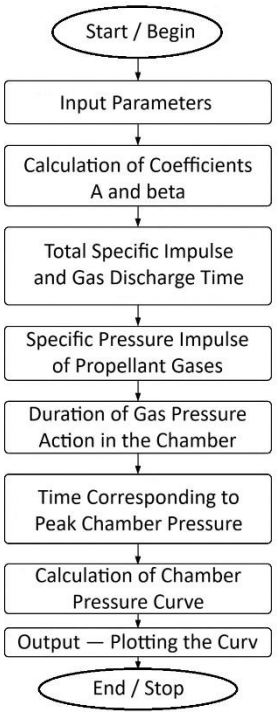


Figure 5. Algorithm of the software solution of Bravin's method

The software solution also enables the calculation of the gas-operating system parameters by simply varying the adopted design parameters. The input quantities used are the barrel caliber, projectile mass, propellant charge mass, bolt mass, initial projectile velocity, maximum propellant gas pressure, the propellant gas pressure at the muzzle and the propellant gas pressure at the gas port location obtained from the internal ballistics calculation, the diameter of the gas port, the piston diameter, the diametral clearance between the piston and the chamber, the initial chamber volume, the reduced barrel length, the projectile travel time from the gas port to the muzzle, the initial return spring force, the return spring stiffness, and the sliding friction coefficient. As output, a diagram of pressure variation in the barrel and in the gas regulator chamber is obtained [8].

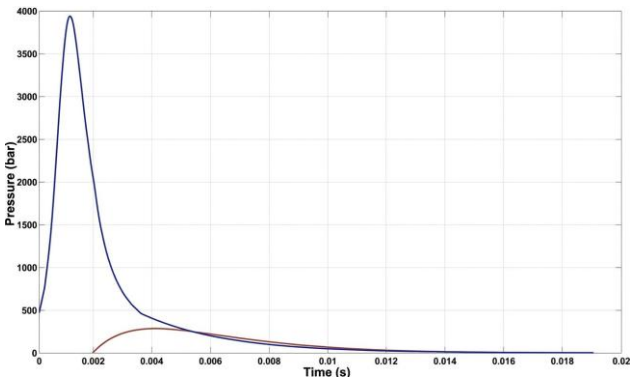


Figure 6. Diagram of pressure variation in the barrel and in the gas regulator chamber.

The obtained pressure variation diagram (Figure 6) correlates with the theoretical diagram shown in Figure 4. The pressure in the chamber begins to rise from the moment t_{k0} = 0.0020 *s*, i.e., when the projectile passes the gas port. The pressure in the barrel is dropping sharply, and at the moment the projectile is at the gas port it equals 2105 *bar*. Based on the diagram, it can be observed that the pressure in the chamber rises more slowly than the pressure in the barrel and is maintained long enough to ensure reliable operation of the automatics even when the barrel pressure is lower. It reaches its maximum value p_{km} = 284 *bar*. The total duration of the propellant gas action in the chamber is t_k = 0.0188 *s*. The pressure curves in the barrel and chamber nearly coincide and continue to decrease during the period of after-effect of the propellant gases, reaching zero after 0.02 *s*.

3. DYNAMIC ANALYSIS

3.1. Work Cycle Diagram

The work cycle diagram of the automatic mechanism represents a graphical or tabular depiction of the interconnected operating phases that occur during a single shot, i.e., during the entire operating cycle of the weapon. The cycle diagram shows the sequence, duration, and overlap of individual processes. Essentially, the cycle diagram is a schematic model of the working process, serving as a basis for studying, designing, and improving the weapon.

For the purpose of researching the operation of the automatics of the 30 mm automatic cannon, a high-speed camera was used, the *Phantom v1212.* The use of a high-speed camera represents one of the key methods for the nonlinear analysis of part motion in real time. Given that the bolt's operating cycle takes place within fractions of a second, standard measurement methods often cannot capture the critical moments that define phase changes. Based on the high-resolution recordings, a work cycle diagram of the 30 mm automatic cannon was constructed (Table 1). The masses of the automatic mechanism's elements are shown in Table 2.

Table 1. Work cycle diagram of the 30 mm automatic cannon

Phases	No.	Motion of parts	Travel distance (*mm*)	Time (*s*)	Mass (*kg*)
Recoil	1	Unlocking	0-35	0.01	m1+m7+ m6
	2	Joint motion	35-350	0.02	m3+m4+ m6+m7
	3	Impact on case ejector	350		
	4	Case ejection	350-400	0.006	m3+m6+ m7
	5	Impact on buffer	400		
	6	Buffer compression and end of recoil	400-420	0.004	m1+m2+ m6+m7
Counter-recoil Phases	1	Joint motion	420-390	0.05	m1+m2+ m6+m7
	2	Impact of bolt on case head	390		
	3	Joint motion	390-35	0.04	m3+m5+ m6+m7
	4	Impact of bolt on rear of barrel	35		

Table 2. Masses of the automatic mechanism's elements

Bolt carrier	m1
Bolt	m2
Bolt assembly	m3
Case	m4
Cartridge	m5
Piston	m6
Return spring	m7

4. BOLT MOTION KINEMATICS

In the paper, a model of the kinematics of the motion of the bolt of the 30 mm automatic cannon was developed using code, focusing on the multi-phase dynamics during the recoil and counter-recoil cycle. The model uses the real propellant gas pressure profile in the gas chamber as input to the dynamic model of the motion of the bolt assembly.

The simulation is based on the numerical solution of a system of second-order differential equations describing the motion of the bolt as a function of time. The complete cycle is divided into seven discrete phases, where each phase has a defined displacement length, the action of the propellant gas force, and the influence of the buffer. For each phase, the ODE system is solved separately using the function *ode45*, using an *event* -function for automatic detection of the end of the phase. This achieves a modular and physically consistent simulation [9].

The input pressure *pk(t)* is loaded from a *.mat* file obtained from the previous calculation of the pressure in the gas cylinder and is interpolated in time. The dynamics of the bolt include the effect of the spring, friction, and buffer, with parameters defined according to the technical characteristics of the system. The recoiling mass dynamically changes in the corresponding phases depending on the mechanical state (presence of the cartridge, case, etc.).

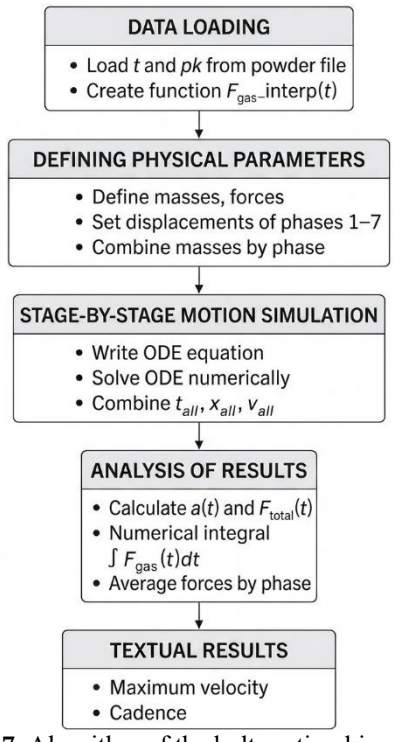


Figure 7. Algorithm of the bolt motion kinematics

Based on the numerical results, the key values of the system were calculated, including the maximum bolt velocity and the rate of fire.

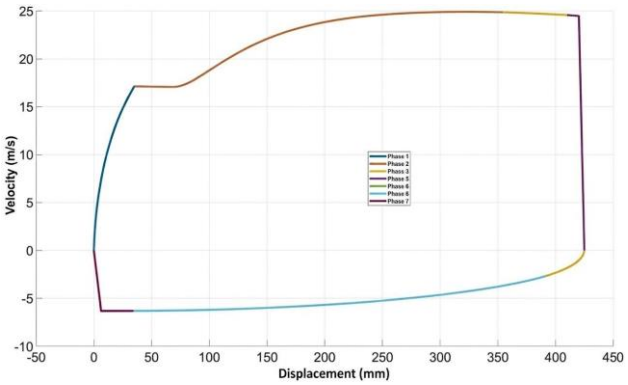


Figure 8. Bolt velocity as a function of position (V=f(x)).

The first phase represents the unlocking of the bolt. In this phase, the propellant gases exert the greatest influence on the system. The velocity of the bolt carrier increases sharply, and the diagram shows that the maximum acceleration occurs precisely here. This phase is crucial for the initial actuation of the mechanism and confirms that the gas profile correctly transfers energy to the piston.

After the initial acceleration and unlocking, the second phase involves extraction of the case, during which the entire bolt assembly together with the case joins the recoiling mass. Based on the diagram in Figure 9 and 10, a brief interval of constant bolt-assembly velocity can be observed at the very beginning of the second phase. This occurrence is a consequence of the sudden increase in inertial mass. Namely, the propellant gas pressure at that moment acts on a mass approximately three times greater than in the initial phase of motion. Thereafter, the velocity remains high but stable, while the gas force gradually decreases. The second phase ensures continuity of motion and shows that the system has enough energy to overcome the inertia of the bolt mass.

In the third phase, the gas impulse ceases, and the bolt continues its motion owing to the accumulated energy. The velocity decreases, and the average force is smaller. In this phase, the ejection of the case occurs which additionally slows the system down and represents a real mechanical effect in the operation of the weapon.

In the fourth phase, the bolt strikes the buffer. This phase clearly shows the dissipation of energy. The bolt velocity decreases, and the buffer absorbs the impact, which is seen through the sudden drop in force.

The bolt then comes to a temporary stop, which is reflected in the negative velocity values. The fifth phase provides a brief pause in the cycle and enables mechanical preparation for the return stroke. The diagram shows that the forces in this phase are negative, which is a consequence of the return action of the spring.

The longest phase of the return motion is the motion of the bolt together with the cartridge. The velocity is negative and stable, and the average forces indicate the dominant influence of spring and friction. This phase is crucial for chambering the next cartridge and preparing for the

following cycle.

The final phase represents the locking of the bolt. The bolt completes its return motion and assumes its initial position. The velocity decreases toward zero. This phase ensures the stabilization of the system and prepares it for the next firing cycle.

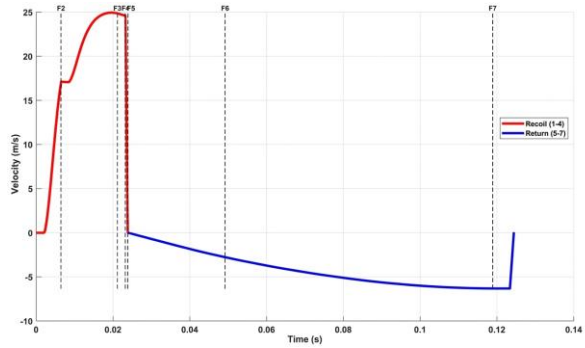


Figure 9. Variation of bolt velocity as a function of time (V=f(s)).

Analysis of the diagrams and tables confirms that the bolt dynamics proceed in accordance with the expected physical principles. The obtained rate of fire of 482 *rounds/min* shows a relative deviation of ~5%, compared to the know value. The diagram of bolt velocity variation, with a maximum value of 24.92 *m/s*, is free of sudden oscillations that could lead to dynamic overloads, which indicates stable operation of the system.

5. CONCLUSION

Based on the available data on the 30 mm automatic cannon and the 30×173 mm cartridge, dynamic analysis of 30 mm automatic cannon operating mechanism was performed.

The internal ballistics calculation was performed using the Drozdov method, and after optimization, the maximum propellant gas pressure in the barrel of the 30 mm automatic cannon was obtained as P_m=*394 MPa,* while the muzzle velocity of the projectile is V_0=*1104 m/s.*

Starting from the conditions of the set task, the method of theoretical examination of propellant gas pressures in gas-operating devices according to Bravin's method was considered. The resulting pressure curve in the gas cylinder fully correlates with the theoretical and experimental work in this field. The maximum pressure value in the chamber is p_{km}=*283.76 bar*, the duration of the propellant gas action in the chamber is t_k=*0.0188 s*, and the time corresponding to the maximum pressure in the chamber is t_{km}=*0.0021 s.*

Based on the constructed work cycle diagram of the 30 mm automatic cannon, a simulation of the bolt motion through seven phases with variable masses was performed, using numerical integration by means of the *ode45* method. The previously obtained pressure curve in the chamber was used as the input data. The displacement and velocity diagrams by phase show that the greatest acceleration occurs in the first phases (1–2), when the gases act directly on the piston and the bolt carrier. In phase 3, the force and velocity decrease due to the resistance of case extraction, while phase 4 clearly shows the dissipation of energy through the buffer. The return phases (5–7) are characterized by negative velocity, confirming the correct return of the bolt to its initial position. This distribution confirms that the model successfully captures the transition between recoil and counter-recoil, and that the buffer plays a key role in stabilizing the system. A rate of fire of 482 rounds per minute was obtained, which deviates from the experimental value by ~5%, confirming that the simulation faithfully describes the real operation of the bolt. Each phase has a clearly defined dynamic, ranging from the initial acceleration under the gas impulse, through energy dissipation in the buffer, to the return motion and stabilization by locking of the bolt. The obtained results are consistent with the expected mechanical behavior and represent a reliable basis for further optimization of the design.

Further improvements to the simulation could be achieved by introducing spring nonlinearities for a more realistic representation of the elastic forces, as well as by applying different loss coefficients in the gas system. In addition, instead of idealized viscous friction, a real friction model that better reflects the actual mechanical operating conditions should be introduced. Finally, extending the simulation to a multi-cycle regime, instead of a single-cycle one, would enable the analysis of the system's durability, stability, and reliability under conditions of intensive use.

Acknowledgement

This work was supported by the Ministry of science, technological development and innovations (Serbia), Contract No. 451-03-34/2026-03/200325.

References

[1] Petrović M.: Mehanika automatskog oružanja (Mechanics of Automatic Weapons), Media Center "Odbrana", Belgrade, 2009.

[2] V. D. Tien, M. Macko, S. Procházka, V. V. Bien, Mathematical Model of a Gas-Operated Machine Gun, Advances in Military Technology, vol. 17, no. 1, pp. 63–77, 2022.

[3] Petrović M., Kari A.: Zbirka zadataka iz mehanike naoružanja 2 (Collection of Problems in Weapon Mechanics 2), Military Academy, Belgrade, 2010.

[4] Ristić Z.: Zbirka zadataka iz mehanike naoružanja (Collection of Problems in Weapon Mechanics), VIZ – Printing and Reproduction Section, Belgrade, 2004.

[5] Cvetković M.: Unutrašnja balistika (Internal Ballistics), Military Publishing Institute, Belgrade, 1998.

[6] Tančić Lj.: Zbirka zadataka iz unutrašnje balistike (Collection of Problems in Internal Ballistics), Military Academy, Belgrade, 1997.

[7] Bravin E.L., Strelkovoe pušečnoe vooruženie samoletov, Moskva, 1941.

[8] Radovanovic N., Kari A.: Analysis of Construction Parameters of Gas Operated Weapons, OTEH, pp. 116–121, Belgrade, 2018.

[9] P. D. Nguyen, B. V. Vo, M. N. Nguyen, and H. T. Tran, "Dynamics of Automatic Firing System Type Gas-Operated Weapon," Problemy Mechatroniki: uzbrojenie, lotnictwo, inżynieria bezpieczeństwa, vol. 14, no. 4, pp. 9–22, 2023.